AIP | Physics of Plasmas

Modulation instability and dissipative rogue waves in ion-beam plasma: Roles of ionization, recombination, and electron attachmenta)

Shimin Guo and Liquan Mei

Citation: Physics of Plasmas (1994-present) **21**, 112303 (2014); doi: 10.1063/1.4901037
View online: http://dx.doi.org/10.1063/1.4901037
View Table of Contents: http://scitation.aip.org/content/aip/journal/pop/21/11?ver=pdfcov
Published by the AIP Publishing

Modulation instability and dissipative rogue waves in ion-beam plasma: Roles of ionization, recombination, and electron attachment[a)]

Shimin Guo[b)] and Liquan Mei[c)]
School of Mathematics and Statistics, Xi'an Jiaotong University, Xi'an 710049, China

(Received 21 July 2014; accepted 23 October 2014; published online 11 November 2014)

The amplitude modulation of ion-acoustic waves is investigated in an unmagnetized plasma containing positive ions, negative ions, and electrons obeying a kappa-type distribution that is penetrated by a positive ion beam. By considering dissipative mechanisms, including ionization, negative-positive ion recombination, and electron attachment, we introduce a comprehensive model for the plasma with the effects of sources and sinks. Via reductive perturbation theory, the modified nonlinear Schrödinger equation with a dissipative term is derived to govern the dynamics of the modulated waves. The effect of the plasma parameters on the modulation instability criterion for the modified nonlinear Schrödinger equation is numerically investigated in detail. Within the unstable region, first- and second-order dissipative ion-acoustic rogue waves are present. The effect of the plasma parameters on the characteristics of the dissipative rogue waves is also discussed.
 [http://dx.doi.org/10.1063/1.4901037]

I. INTRODUCTION

Recently, plasma systems with high-energy ion beam have attracted considerable attention because of their wide range of potential applications in plasma lenses, heavy-ion fusion, and cosmic ray propagation.[1,2] The presence of such ion beams can significantly modify the collective behavior in plasmas[3,4] and introduce ion-ion instability.[5] Spacecraft observations indicate that electron and ion beams can drive broadband electrostatic waves in the Earth's plasma sheet boundary layer.[6] Moreover, solitary waves with negative potential have been observed in the vicinity of the ion-beam region of the auroral zone.[7] When an ion beam penetrates into an unmagnetized plasma with ion motion, three normal modes[8] can propagate in the system: plasma ion-acoustic waves, fast ion-beam modes, and slow ion-beam modes. The behavior and characteristics of these electrostatic modes have been theoretically investigated[9–13] and experimentally established[5,14,15] in ion-beam plasmas.

Negative ions are ubiquitous in space environments as well as in laboratory plasmas. They have been found in the D- and F-regions of the Earth's ionosphere,[16] neutral beam sources, and plasma processing reactors.[17] Because of elementary processes, such as dissociative and nondissociative electron attachment to neutrals,[18] negative ions can appear in electronegative plasmas. Because the presence of negative ions can significantly modify the electron-energy-distribution function and charged species balance, many investigations have been performed on plasmas with negative ions.[11,19,20]

In most previous studies, unspecified sources and sinks were not taken into account in the conservation equations. However, the mechanisms, including ionization and recombination, are density-dependent processes, which means that the collective behavior in the system can be strongly affected. For example, plasma particles are continuously being created by ionization in real laboratory devices, such as gas discharge devices.[18] These particles are also lost by volume recombination, which takes place in the same time scale as ionization. Therefore, it is important to investigate the effect of these relevant processes on the collective behavior in plasma systems.[21–23]

It is well-known that the velocity distribution of electrons has a great influence on wave motions in plasmas. In the past few decades, the classical Maxwellian particle distribution has been the most commonly used velocity distribution. However, energetic (superthermal) particles that depart from the Maxwellian distribution can occur because of the effect of external forces or wave-particle interactions.[24] Because of the presence of superthermal electrons, a high-energy tail appears in the distribution function, which can be modeled by a kappa-type distribution.[25] The kappa-type distribution can provide a powerful framework for the analysis of real data in space plasma environments. For example, theoretical analysis with $\kappa = 4$ is in good agreement with the electron distribution observed in the solar wind.[26] Note that, the Maxwellian distribution can be recovered from the kappa-type distribution when $\kappa \to \infty$. Although some studies have been performed on the link between the kappa-type distribution and the Tsallis distribution,[27] this analogy still appears to be a controversial topic.

Recently, understanding the origin of rogue waves in plasma physics has become a hot topic because of fundamental scientific interest and the complex mechanisms involved in its formation. A rogue wave, also known as an extreme wave, freak wave, or killer wave, is a single, rare, and high-energy event appearing in the ocean.[28] The appearance of a rogue wave is mainly because of the modulation instability, where instability induced from a small external perturbation of a plane wave has the possibility to create a very high

[a)]The project was supported by NSF of China (11371289, 11371288) and China Postdoctoral Science Foundation (2014M560756).
[b)]E-mail: gsm861@126.com
[c)]E-mail: lqmei@mail.xjtu.edu.cn

amplitude wave that eventually "disappears without a trace."[29,30] An important mathematical model for the rogue wave is the rational solution of the nonlinear Schrödinger (NLS) equation in the unstable region. The features of rogue waves have been theoretically investigated in many plasma systems[31–38] and confirmed in experiments.[39,40]

The aim of this paper is to investigate the propagation of rogue waves in an ion-beam plasma containing negative ions, positive ions, and superthermal electrons with a kappa-type distribution. We take into account dissipative mechanisms, including ionization, negative-positive ion recombination, and electron attachment, in the plasma model. This paper is organized as follows. In Sec. II, we present the theoretical model and derive the modified NLS equation with a linear dissipative term via the reductive perturbation technique. In Sec. III, we discuss the basic features of modulation instability and nonlinear structures of dissipative ion-acoustic rogue waves. Finally, conclusions are given in Sec. IV.

II. THEORETICAL MODEL AND MODIFIED NLS EQUATION

Consider a one-dimensional unmagnetized plasma consisting of four components: superthermal electrons, positive ions, negative ions, and a positive ion beam. Because the thermal speed of electrons is much larger than that of ions, we ignore electron inertia and assume that electrons satisfy a kappa-type distribution. For simplicity, we also assume that the creation of negative ions is because of electron attachment. In our system, we also consider the ionization of neutral gas by fast electrons and positive-negative ion recombination. Here, our plasma model is based on a set of fluid equations for the ion beam, positive ions, and negative ions.

For positive ions, the normalized evolution equations are

$$\frac{\partial n_p}{\partial t}+\frac{\partial(n_p u_p)}{\partial x}=\nu_{ion}n_e-\nu_{rec}n_p n_n, \tag{1}$$

$$\frac{\partial u_p}{\partial t}+u_p\frac{\partial u_p}{\partial x}=-\frac{\partial \Phi}{\partial x}. \tag{2}$$

For negative ions, they are

$$\frac{\partial n_n}{\partial t}+\frac{\partial(n_n u_n)}{\partial x}=\nu_{att}n_e-\nu_{rec}n_p n_n, \tag{3}$$

$$\frac{\partial u_n}{\partial t}+u_n\frac{\partial u_n}{\partial x}=\alpha\frac{\partial \Phi}{\partial x}. \tag{4}$$

For the ion beam, they are

$$\frac{\partial n_b}{\partial t}+\frac{\partial(n_b u_b)}{\partial x}=0, \tag{5}$$

$$\frac{\partial u_b}{\partial t}+u_b\frac{\partial u_b}{\partial x}=-\beta\frac{\partial \Phi}{\partial x}. \tag{6}$$

The above six equations are coupled by the Poisson equation

$$\frac{\partial \Phi^2}{\partial x^2}=n_e+\mu_n n_n-\mu_b n_b-\mu_p n_p. \tag{7}$$

The normalized electron distribution is given by

$$n_e=\left(1-\frac{\Phi}{\kappa-3/2}\right)^{-\kappa+1/2}, \tag{8}$$

where κ is a real parameter measuring the deviation from the standard Maxwellian equilibrium. Note that the condition $\kappa>3/2$ should be satisfied for a physically meaningful thermal speed. In Eqs. (1)–(8), ν_{ion} is the rate of ionization, ν_{rec} is the rate of positive-negative ion recombination, and ν_{att} is the rate of the electron attachment to the neutrals resulting in the creation of negative ions. In addition, $n_j(j=p,n,b,$ or e for positive ions, negative ions, the ion beam, or electrons, respectively) represents the number density of j-species particles normalized by their equilibrium values n_{j0}. $u_j(j=p,n,$ or $b)$ represents the velocity of j-species particles normalized by the positive ion-acoustic speed $C_s=(\kappa_B T_e/m_p)^{1/2}$. The electrostatic potential Φ, time t, and space x are normalized by the thermal potential $\kappa_B T_e/e$, inverse ion plasma frequency $\omega_{pi}^{-1}=(4\pi n_{p0}e^2/m_p)^{-1/2}$, and Debye length $\lambda_D=(\kappa_B T_e/4\pi n_{p0}e^2)^{1/2}$, respectively. Here, κ_B is the Boltzmann constant, T_e is the electron temperature, e is the magnitude of the electron charge, $\alpha=m_p/m_n$, and $\beta=m_p/m_b$. The overall charge neutrality condition, $n_{e0}+n_{n0}=n_{p0}+n_{b0}$, implies that $1+\mu_n=\mu_p+\mu_b$ with $\mu_n=n_{n0}/n_{e0}$, $\mu_p=n_{p0}/n_{e0}$, and $\mu_b=n_{b0}/n_{e0}$.

To investigate the propagation characteristics of the nonlinear ion-acoustic waves in the short-wavelength limit by the reductive perturbation method,[41] we introduce the following slow space and time scales:

$$\xi=\epsilon(r-Vt),\ \tau=\epsilon^2 t, \tag{9}$$

where V is the group velocity, which will be determined later, and $0<\epsilon\ll 1$ is a small ordering parameter.

The dependent variables are expanded as follows:

$$\begin{aligned}
[n_p,n_n,n_b]&=1+\sum_{m=1}^{\infty}\epsilon^m\sum_{l=-\infty}^{+\infty}[n_{pl}^{(m)}(\xi,\tau),n_{nl}^{(m)}(\xi,\tau),n_{bl}^{(m)}(\xi,\tau)]e^{il(kx-\omega t)},\\
[u_p,u_n,u_b]&=\sum_{m=1}^{\infty}\epsilon^m\sum_{l=-\infty}^{+\infty}[u_{pl}^{(m)}(\xi,\tau),u_{nl}^{(m)}(\xi,\tau),u_{lb}^{(m)}(\xi,\tau)]e^{il(kx-\omega t)},\\
\Phi&=\sum_{m=1}^{\infty}\epsilon^m\sum_{l=-\infty}^{+\infty}\Phi_l^{(m)}(\xi,\tau)e^{il(kx-\omega t)}.
\end{aligned} \tag{10}$$

Here, $i = \sqrt{-1}$ and the real parameters k and ω are the fundamental (carrier) wave number and frequency, respectively. Because the variables n_j, $u_j (j = p, n,$ or $b)$, and Φ are real, the coefficients in Eq. (10) should satisfy the condition $A_{-l}^{(m)} = A_l^{(m)*}$, where the asterisk denotes the complex conjugate.

Because the rate of ionization, the rate of positive-negative ion recombination, and the rate of electron attachment are small compared with the ion oscillation frequency, we assume that $\nu_{ion} \sim O(\epsilon^2)$, $\nu_{rec} \sim O(\epsilon^2)$, and $\nu_{att} \sim O(\epsilon^2)$ in the following calculations. The reasons why we chose the second-order perturbations for the dissipative terms are (i) choosing the second-order perturbations can include the effects of the dissipative mechanisms in the linear dissipative term of the modified NLS equation, and (ii) the second-order perturbations of the dissipative terms are consistent with the nonlinear perturbations of Eqs. (9) and (10).

Substituting Eqs. (9) and (10) into Eqs. (1)–(8) and collecting the terms in different orders of ϵ, we can obtain the m th order reduced equations. The first-order ($m = 1$) equations with $l = 1$ can be expressed in the following matrix form:

$$\begin{aligned}\left[n_{p1}^{(1)}, n_{n1}^{(1)}, n_{b1}^{(1)}\right]^{\mathrm{T}} &= \left[\frac{k^2}{\omega^2}, -\frac{\alpha k^2}{\omega^2}, \frac{\beta k^2}{\omega^2}\right]^{\mathrm{T}} \Phi_1^{(1)},\\ \left[u_{p1}^{(1)}, u_{n1}^{(1)}, u_{b1}^{(1)}\right]^{\mathrm{T}} &= \left[\frac{k}{\omega}, -\frac{\alpha k}{\omega}, \frac{\beta k}{\omega}\right]^{\mathrm{T}} \Phi_1^{(1)},\end{aligned} \tag{11}$$

where T denotes the transpose of the matrix. We can also obtain the following dispersion relationship:

$$\frac{k^2}{\omega^2} = \frac{-\mu_b k^2 \beta - \mu_p k^2 + c_1 \omega^2 + k^2 \omega^2}{\omega^2 \alpha \mu_n}, \tag{12}$$

where $c_1 = (2\kappa - 1)/(2\kappa - 3)$. Figure 1 shows the variation of wave frequency ω with wave number k for different values of spectral index κ, ion beam to electron density ratio μ_b, and negative ion to electron density ratio μ_n. Plot (a) shows that the wave frequency ω increases with decreasing superthermal particle excess, where the Maxwellian distribution is approached. This is because the nonthermality of the plasma can reduce the plasma screening length.[44] From plot (b), increasing the value of μ_b can decrease the wave frequency ω, while the opposite effect is observed for increasing μ_n (plot (c)).

From the second-order ($m = 2$) reduced equations with $l = 1$, we obtain the following corrections of the first-order quantities:

$$\begin{aligned}\left[n_{p1}^{(2)}, n_{n1}^{(2)}, n_{b1}^{(2)}\right]^{\mathrm{T}} &= \left[-\frac{ik}{\omega^3}, \frac{\alpha ik}{\omega^3}, -\frac{\beta ik}{\omega^3}\right]^{\mathrm{T}}\\ &\quad\times\left((-2Vk + 2\omega)\frac{\partial \Phi_1^{(1)}}{\partial \xi} + ik\omega\Phi_1^{(2)}\right),\\ \left[u_{p1}^{(2)}, u_{n1}^{(2)}, u_{b1}^{(2)}\right]^{\mathrm{T}} &= \left[-\frac{i}{\omega^2}, \frac{\alpha i}{\omega^2}, -\frac{\beta i}{\omega^2}\right]^{\mathrm{T}}\\ &\quad\times\left((-Vk + \omega)\frac{\partial \Phi_1^{(1)}}{\partial \xi} + ik\omega\Phi_1^{(2)}\right),\end{aligned} \tag{13}$$

and the compatibility condition

$$V = \sqrt{\frac{(\mu_b \beta + \mu_p + \alpha\mu_n)c_1^2}{(c_1 + k^2)^3}}. \tag{14}$$

Recall that the above equation is the expression for the group velocity V without the vector sign, which is defined in terms of speed. For the next order ($m = 2$ and $l = 2$), we obtain the following reduced equations:

$$\begin{aligned}&[n_{p2}^{(2)}, n_{n2}^{(2)}, n_{b2}^{(2)}, u_{p2}^{(2)}, u_{n2}^{(2)}, u_{b2}^{(2)}, \Phi_2^{(2)}]^{\mathrm{T}}\\ &\quad= [\Delta_1, \Delta_2, \Delta_3, \Delta_4, \Delta_5, \Delta_6, \Delta_7]^{\mathrm{T}}(\Phi_1^{(1)})^2.\end{aligned} \tag{15}$$

Here, the coefficients $\Delta_1 - \Delta_7$ are expressed in the Appendix.

Because of the nonlinear self-interaction of the carrier waves, the second-order ($m = 2$) quantities with the zeroth harmonic modes ($l = 0$) can be given by

$$\begin{aligned}&[n_{p0}^{(2)}, n_{n0}^{(2)}, n_{b0}^{(2)}, u_{p0}^{(2)}, u_{n0}^{(2)}, u_{b0}^{(2)}, \Phi_0^{(2)}]^{\mathrm{T}}\\ &\quad= [\Delta_8, \Delta_9, \Delta_{10}, \Delta_{11}, \Delta_{12}, \Delta_{13}, \Delta_{14}]^{\mathrm{T}}|\Phi_1^{(1)}|^2,\end{aligned} \tag{16}$$

where $\Delta_8 - \Delta_{14}$ are given in the Appendix.

Finally, substituting Eqs. (11)–(16) into the third-order ($m = 3$) relationship with the first harmonic mode ($l = 1$), we obtain an explicit compatibility condition, i.e., the modified NLS equation with a linear dissipative term in the following form:

$$i\frac{\partial \Phi}{\partial \tau} + P\frac{\partial^2 \Phi}{\partial \xi^2} + Q|\Phi|^2\Phi + i\Upsilon\Phi = 0, \tag{17}$$

where $\Phi = \Phi_1^{(1)}$. The dispersion coefficient P, the nonlinear coefficient Q, and the dissipative coefficient Υ are given by

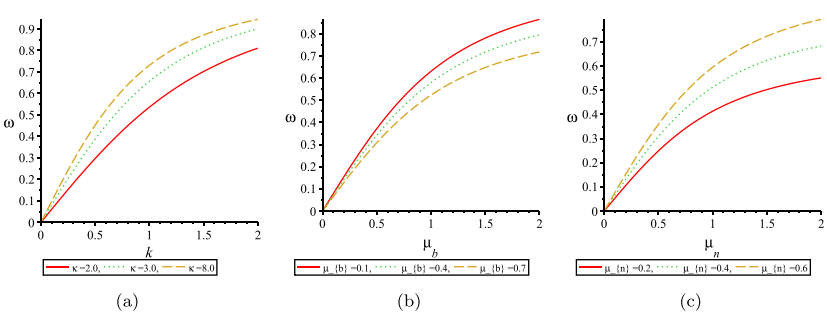

FIG. 1. Variation of wave frequency ω with wave number k for different values of (a) κ, (b) μ_b, and (c) μ_n. The parameters are (a) $\alpha = 0.6$, $\beta = 0.9$, $\nu_{ion} = \nu_{att} = \nu_{rec} = 0.01$, $\mu_b = 0.6$, and $\mu_n = 0.2$, (b) $\alpha = 0.25$, $\beta = 0.35$, $\nu_{ion} = \nu_{att} = \nu_{rec} = 0.01$, $\kappa = 3.5$, and $\mu_n = 0.15$, (c) $\alpha = \beta = 0.2$, $\nu_{ion} = \nu_{att} = \nu_{rec} = 0.01$, $\kappa = 4.5$, and $\mu_b = 0.85$.

$$P = \frac{1}{2}\frac{\partial^2\omega}{\partial k^2} = -\frac{3k(\mu_b\beta + \mu_p + \mu_n\alpha)c_1}{2\sqrt{(c_1+k^2)(\mu_b\beta+\mu_p+\mu_n\alpha)}(c_1+k^2)^2},$$

$$Q = \frac{1}{2k^2(\mu_b\beta+\mu_p+\mu_n\alpha)}\big[-\mu_p k^2\omega(\Delta_1+\Delta_8) - \mu_n k^2\alpha\omega(\Delta_2+\Delta_9) - \mu_b k^2\beta\omega(\Delta_3+\Delta_{10})$$
$$-2\mu_p k^3(\Delta_4+\Delta_{11}) - 2\mu_n k^3\alpha(\Delta_5+\Delta_{12}) - 2\mu_b k^3\beta(\Delta_6+\Delta_{13}) + 2\omega^2 c_2(\Delta_7+\Delta_{15})\big],$$

$$\Upsilon = \frac{1}{2k^2(\mu_b\beta+\mu_p+\mu_n\alpha)}\left[\nu_{rec}k^2(\alpha-1)(\mu_n-\mu_p) - \omega^2 c_1(\mu_p\nu_{ion} - \mu_n\nu_{att})\right],$$

where $c_1 = (2\kappa-1)/(2\kappa-3)$, $c_2 = (2\kappa^2-1)/(2\kappa-3)^2$.

III. MODULATION INSTABILITY AND DISSIPATIVE ROGUE WAVES

In this section, we will investigate the modulation instability of ion-acoustic waves and its relevance to the plasma parameters. Then, the first- and second-order dissipative ion-acoustic rogue waves are presented and discussed in the unstable region.

A. Modulation instability

Assume that, because of the presence of the dissipative term, the modified NLS equation (17) allows the following plane-wave solution:

$$\Phi = \Phi_0(\tau)\exp\left[-i\int_0^\tau \delta(\tau)d\tau\right], \tag{18}$$

where $\Phi_0(\tau)$ represents the amplitude of the pump carrier wave, and $\delta(\tau)$ is the nonlinear shift frequency. Substituting the above wave solution into Eq. (17), we obtain the following two equations:

$$\frac{d\Phi_0(\tau)}{d\tau} + \Upsilon\Phi_0(\tau) = 0, \quad \delta(\tau) = -Q|\Phi_0(\tau)|^2. \tag{19}$$

Solving Eq. (19), we obtain

$$\Phi_0(\tau) = \Phi_{00}\exp(-\Upsilon\tau), \;\; \delta(\tau) = -Q|\Phi_{00}|^2\exp(-2\Upsilon\tau),$$

where Φ_{00} is a real constant.

For stability/instability analysis, we consider development of perturbed amplitude $\varphi = \varphi(\xi,\tau)$ ($|\varphi| \ll \Phi_0$) according to

$$\Phi = (\Phi_0(\tau) + \varphi(\xi,\tau))\exp\left[-i\int_0^\tau \delta(\tau)d\tau\right]. \tag{20}$$

Substituting Eq. (20) into the modified NLS equation (17), the perturbation $\varphi(\xi,\tau)$ satisfies the following governing equation:

$$i\frac{\partial\varphi}{\partial\tau} + P\frac{\partial^2\varphi}{\partial\xi^2} + Q|\Phi_0|^2(\varphi+\varphi^*) + i\Upsilon\varphi = 0, \tag{21}$$

where φ^* is the complex conjugate of φ. Substituting the transformations $\varphi = U + iV$, $(U,V) = (U_0,V_0)\exp[i(K\xi - \Omega\tau)]$ into Eq. (21) gives the following nonlinear dispersion:

$$(\Omega + i\Upsilon)^2 = (PK^2)^2\left(1 - \frac{2Q}{P}\frac{|\Phi_0|^2}{K^2}\right). \tag{22}$$

Here, $K(\ll k)$ and $\Omega(\ll\omega)$ are the wave number and frequency of the modulation, respectively.

From the above dispersion relationship (22), the plasma system is stable when $PQ < 0$. In this case, the carrier wave is stable to modulation instability and may propagate in the form of dark-type excitation, i.e., a localized "hole" or "void" amidst a uniform wave energy region.[42] However, when $PQ > 0$ there is a possibility of instability. When both P and Q have the same sign ($PQ > 0$), the instability of the modulated envelope can occur if $K^2 < K_c^2 = \frac{2Q|\Phi_0|^2}{P}$. For the unstable wave packets, the small wave amplitude may increase to a very high amplitude because of external perturbations, which can create "bright" envelope modulated wave packets. These bright-type wave packets can be the stationary soliton, but the NLS-type equations also allow bright soliton solutions that are localized along both the time- and space-directions. In this paper, we investigate the special doubly localized structures of ion-acoustic waves when $PQ > 0$, i.e., the dissipative ion-acoustic rogue waves that can be generated in a relatively small region.

Now, we will discuss the growth rate of the instability for $PQ > 0$. Substituting $\Omega = i\Gamma$ into the dispersion relationship (22) gives

$$(\Gamma + \Upsilon)^2 = (PK^2)^2\left(\frac{2Q}{P}\frac{|\Phi_0|^2}{K^2} - 1\right). \tag{23}$$

Clearly, the growth rate of the instability is given by

$$\Gamma = -\Upsilon + PK^2\sqrt{\left(\frac{2Q}{P}\frac{|\Phi_0|^2}{K^2} - 1\right)}. \tag{24}$$

To obtain the maximum growth rate of the instability, we take the derivative of Eq. (23) with respect to K^2, and set it to zero. Then, we obtain

$$K_{\max} = \left(\frac{Q}{P}\right)|\Phi_0|^2 = \left(\frac{Q}{P}\right)|\Phi_{00}|^2\exp(-2\Upsilon\tau). \tag{25}$$

With the above value of $K_{\max}$, we obtain the following maximum growth rate of the instability:

$$\Gamma_{\max} = \sqrt{2}|Q||\Phi_0|^2 - \Upsilon$$
$$= \sqrt{2}|Q||\Phi_{00}|^2\exp(-2\Upsilon\tau) - \Upsilon. \tag{26}$$

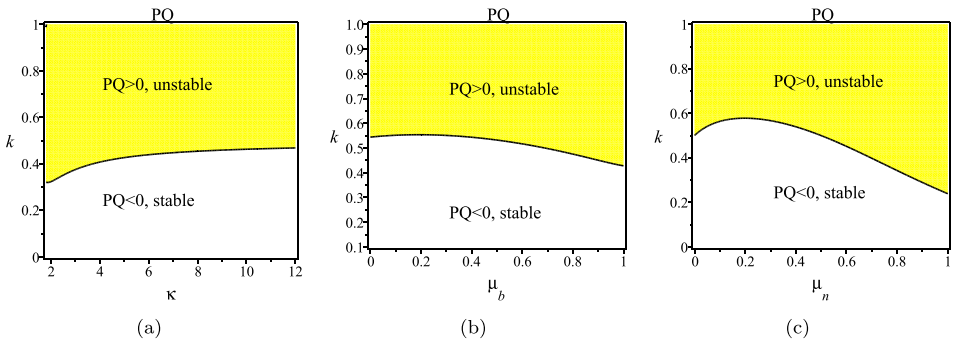

FIG. 2. Contour of the product PQ on the $(\kappa, k)-$, (μ_b, k)-, and $(\mu_n, k)-$ planes. (a) $\alpha = 0.5$, $\beta = 1$, $\nu_{ion} = \nu_{att} = \nu_{rec} = 0.01$, $\mu_b = 0.5$, and $\mu_n = 0.1$. (b) $\alpha = 0.15$, $\beta = 0.45$, $\nu_{ion} = \nu_{att} = \nu_{rec} = 0.01$, $\kappa = 3.0$, and $\mu_n = 0.1$. (c) $\alpha = \beta = 0.1$, $\nu_{ion} = \nu_{att} = \nu_{rec} = 0.01$, $\kappa = 4.0$, and $\mu_b = 0.9$.

From the above discussion, it is important to determine how the plasma parameters influence the product PQ, which determines where the stable ($PQ < 0$) and unstable ($PQ > 0$) regions set in. Figure 2 shows the effects of the parameters κ (the spectral index), μ_b (ion beam to electron density ratio), and μ_n (negative ion to electron density ratio) on the critical wave number threshold k_c when the product PQ changes sign.

(i) Plot (a) shows that increasing the value of κ can lead to an increase of the critical wave number k_c, which changes the unstable region ($PQ > 0$) into the stable region ($PQ < 0$). In other words, an increase of κ can decrease (increase) the unstable (stable) region.

(ii) From plot (b), the effect of μ_b on the stable/unstable region is opposite to that of the parameter κ, i.e., the critical wave number k_c decreases with increasing μ_b. This plot indicates that increasing μ_b can lead to an increase of the modulationally unstable region.

(iii) From plot (c), an increase of μ_n can increase the critical wave number k_c until μ_n reaches a certain value $\mu_n^c \approx 0.18$. Then, a further increase of μ_n can lead to a decrease of k_c. In other words, increasing μ_n can decrease the unstable region if $\mu_n < \mu_n^c$, while increasing μ_n can change $PQ < 0$ (stable case) into $PQ > 0$ (unstable case) if $\mu_n > \mu_n^c$.

B. Dissipative rogue waves

Here, we present and discuss the dissipative ion-acoustic rogue wave solutions of the modified NLS equation (17) within the modulation instability region.

Substituting the new variable[43] $\Psi(\xi, \tau) = \Phi(\xi, \tau)e^{\Upsilon\tau}$ into Eq. (17) gives

$$i\frac{\partial \Psi}{\partial \tau} + P\frac{\partial^2 \Psi}{\partial \xi^2} + Qe^{-2\Upsilon\tau}|\Psi|^2\Psi = 0. \tag{27}$$

Because the dissipative coefficient Υ is very small, we obtain $e^{-2\Upsilon\tau} \approx 1/(1 + 2\Upsilon\tau)$ by the Taylor expansion. Using this approximation, Eq. (27) can be rewritten as

$$i\frac{\partial \Psi}{\partial \tau} + P\frac{\partial^2 \Psi}{\partial \xi^2} + Q\gamma(\tau)|\Psi|^2\Psi = 0, \tag{28}$$

where $\gamma(\tau) = 1/(1 + 2\Upsilon\tau)$. Considering[43]

$$\mathcal{X}(\xi, \tau) = \gamma(\tau)\xi, \quad \mathcal{T} = \gamma(\tau)\tau,$$
$$\hat{\Psi} = \frac{\Psi}{\sqrt{\gamma(\tau)}}\exp\left[i\left(\frac{\Upsilon\gamma(\tau)\xi^2}{2P}\right)\right], \tag{29}$$

we can transform Eq. (28) into the following standard NSL equation:

$$i\frac{\partial \hat{\Psi}}{\partial \mathcal{T}} + P\frac{\partial^2 \hat{\Psi}}{\partial \mathcal{X}^2} + Q|\hat{\Psi}|^2\hat{\Psi} = 0. \tag{30}$$

Using the transformations (29) and the rogue wave solutions of the standard NLS equation (30), we obtain the following approximate dissipative ion-acoustic rogue waves of the modified NLS equation (17):

Case I. The first-order dissipative rogue wave solution

$$\Phi(\xi, \tau) = \sqrt{\frac{2P}{Q}}\left(\frac{4 + 16iP\gamma(\tau)\tau}{1 + 16(P\gamma(\tau)\tau)^2 + 4(\gamma(\tau)\xi)^2} - 1\right) \times \exp\left(-i\left(\frac{\Upsilon\gamma(\tau)\xi^2}{2P}\right)\right)\sqrt{\gamma(\tau)}. \tag{31}$$

Case II. The second-order dissipative rogue wave solution

$$\Phi(\xi, \tau) = \sqrt{\frac{2P}{Q}}\left(1 + \frac{G_2(\xi, \tau) + iK_2(\xi, \tau)}{D_2(\xi, \tau)}\right) \times \exp\left(-i\left(\frac{\Upsilon\gamma(\tau)\xi^2}{2P}\right)\right)\sqrt{\gamma(\tau)}, \tag{32}$$

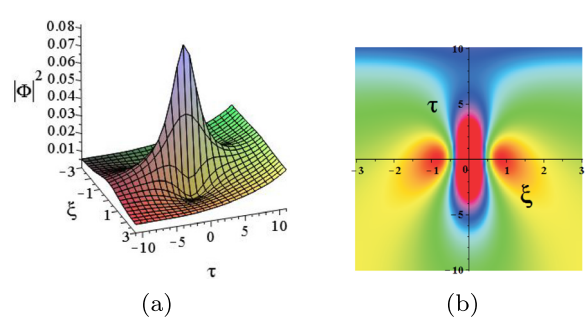

FIG. 3. (a) Wave propagation and (b) density plot for the electronic potential $|\Phi|^2$ of the first-order dissipative ion-acoustic rogue wave solution (31). The parameters are $\alpha = 0.8$, $\beta = 1$, $\mu_b = 0.5$, $\mu_n = 0.1$, $\kappa = 1.8$, $\nu_{ion} = 0.01$, $\nu_{att} = 0.09$, $\nu_{rec} = 0.07$, and $k = 1.2$.

where

$$G_2(\xi,\tau) = -\frac{1}{2}(\gamma(\tau)\xi)^4 - 6(P\xi\tau)^2\gamma^4(\tau) - 10(P\gamma(\tau)\tau)^4 - \frac{3}{2}(\gamma(\tau)\xi)^2 - 9(P\gamma(\tau)\tau)^2 + \frac{3}{8},$$

$$K_2(\xi,\tau) = -P\gamma(\tau)\tau\left[4(P\xi\tau)^2\gamma^4(\tau) + 4(P\gamma(\tau)\tau)^4 + (\gamma(\tau)\xi)^4 - 3(\gamma(\tau)\xi)^2 + 2(P\gamma(\tau)\tau)^2 - \frac{15}{4}\right],$$

$$D_2(\xi,\tau) = \frac{1}{12}(\gamma(\tau)\xi)^6 + \frac{1}{2}(\gamma(\tau)\xi)^4(P\gamma(\tau)\tau)^2 + \frac{2}{3}(P\gamma(\tau)\tau)^6 + \frac{1}{8}(\gamma(\tau)\xi)^4 + \frac{9}{2}(P\gamma(\tau)\tau)^4 + \frac{9}{16}(\gamma(\tau)\xi)^2 + \frac{33}{8}(P\gamma(\tau)\tau)^2 + \frac{3}{32} + (\gamma(\tau)\xi)^2(P\gamma(\tau)\tau)^4 - \frac{3}{2}(P\xi\tau)^2\gamma^4(\tau).$$

In Figures 3 and 4, we show the first- and second-order dissipative ion-acoustic rogue waves with $\Upsilon < 0$ (the forced case), respectively. From these plots, the first- and second-order dissipative rogue waves are localized in both the τ and ξ directions, i.e., they appear from nowhere and disappear without trace.[29] This feature means that the dissipative rogue waves can also concentrate the energy of the plasma system in a small region. Unlike classical rogue waves, from these two figures the nonzero backgrounds of the waves increase because of the presence of the forcing dissipative term. However, the backgrounds of the waves decrease when $\Upsilon > 0$ (the damped case). For simplicity, we do not include the figures here.

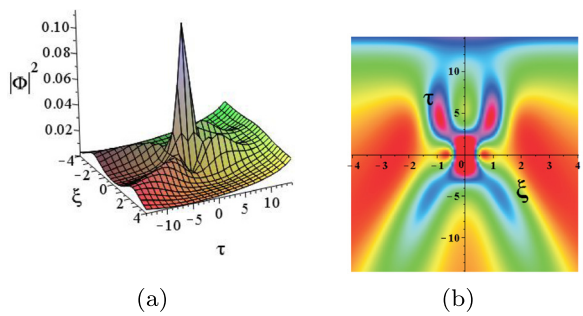

FIG. 4. (a) Wave propagation and (b) density plot for the electronic potential $|\Phi|^2$ of the second-order dissipative ion-acoustic rogue wave solution (32). The parameters are the same as in Fig. 3.

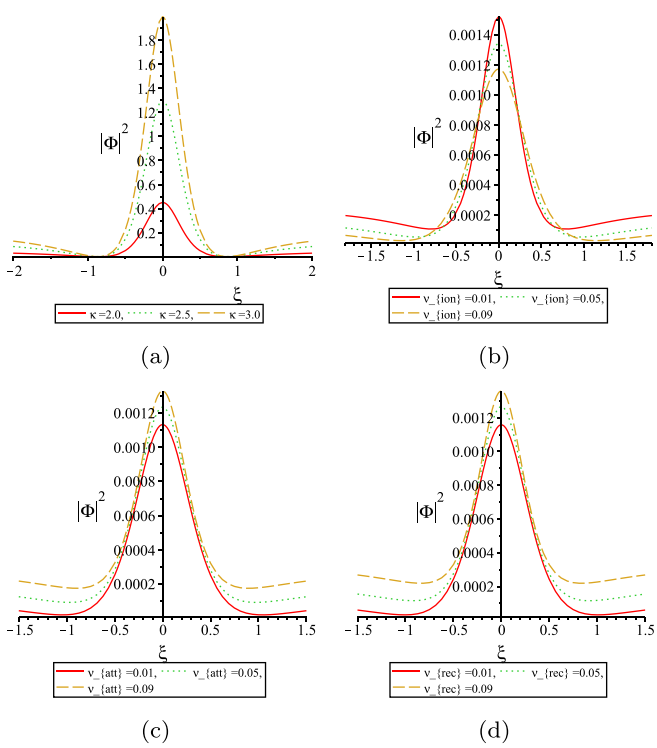

FIG. 5. Variation of the first-order dissipative ion-acoustic rogue wave solution (31) for different values of (a) κ, (b) ν_{ion}, (c) ν_{att}, and (d) ν_{rec}. The parameters are $\alpha = 0.1$, $\beta = 1$, $\mu_b = 0.5$, $\mu_n = 0.3$, (a) $\nu_{ion} = 0.05$, $\nu_{att} = 0.02$, $\nu_{rec} = 0.06$, and $\tau = 0$, (b) $\nu_{att} = 0.02$, $\nu_{rec} = 0.06$, $\kappa = 1.55$, and $\tau = 8$, (c) $\nu_{ion} = 0.05$, $\nu_{rec} = 0.06$, $\kappa = 1.55$, and $\tau = 10$, and (d) $\nu_{ion} = 0.05$, $\nu_{att} = 0.02$, $\kappa = 1.55$, and $\tau = 10$.

From Figure 5, the first-order dissipative ion-acoustic rogue wave solution expressed by Eq. (31) is significantly affected by variations of spectral index κ, the rate of ionization ν_{ion}, the rate of negative-positive ion recombination ν_{rec}, and the rate of electron attachment ν_{att}.

(i) Plots (a), (c), and (d) indicate that the amplitude of the dissipative rogue wave increases with increasing κ, ν_{att}, and ν_{rec} values. This means that increasing the values of these three parameters can enhance the nonlinearity of the plasma system and concentrate the energy in a small region, which increases the amplitude of the pulses.

(ii) Increasing the value of ν_{ion} can decrease the amplitude of the dissipative rogue wave (plot (b)). This behavior can be interpreted as an increase of ν_{ion} can reduce the nonlinearity of the system, so the pulses of the dissipative rogue wave become shorter.

IV. CONCLUSIONS

In summary, we investigated dissipative ion-acoustic waves in an unmagnetized plasma consisting of positive ions, negative ions, an ion beam, and electrons obeying a kappa-type distribution. Dissipative mechanisms, including ionization, negative-positive ion recombination, and electron attachment, were considered in the model. The modified NLS equation with a linear dissipative term was derived by reductive perturbation theory. The effects of the spectral index κ, ion beam to electron density ratio μ_b, and negative ion to electron density ratio μ_n on the wave dispersion and stable/unstable region were discussed in detail.

In the unstable region, dissipative ion-acoustic waves with doubly localized structures can be created because of modulation instability. Our investigation revealed that the amplitude of the dissipative ion-acoustic rogue wave increases with increasing spectral index κ, increasing rate of negative-positive ion recombination ν_{rec}, and increasing rate of

electron attachment ν_{att}. Increasing the values of these three plasma parameters enhances the nonlinearity of the system. However, increasing the rate of ionization ν_{ion} can decrease the nonlinearity of the system and make the pulses shorter.

Our theoretical investigations provide a better understanding of the excitation of rogue waves in laboratory experiments and spatial observations.

ACKNOWLEDGMENTS

The authors express their sincere thanks to the editor and referee for their valuable comments that led to an improved version of the manuscript.

APPENDIX: EXPRESSIONS OF THE COEFFICIENTS

$$\Delta_1 = \frac{k^2}{2\omega^4\mathcal{A}}\left(-3\mu_n k^4\alpha^2 + 3\mu_b k^4\beta^2 - 2c_2\omega^4 - 3\mu_b k^4\beta + 3k^2\omega^2 c_1 + 12k^4\omega^2 - 3\mu_n k^4\alpha\right),$$

$$\Delta_2 = \frac{k^2\alpha}{2\omega^4\mathcal{A}}\left(-3\,\mu_b\,k^4\beta^2 - 3\,\mu_p\,k^4 + 2\,c_2\,\omega^4 - 3\,k^4\alpha\,\mu_b\,\beta - 3\,k^4\alpha\,\mu_p + 3\,k^2\alpha\,\omega^2 c_1 + 12\,k^4\alpha\,\omega^2\right),$$

$$\Delta_3 = \frac{k^2\beta}{2\omega^4\mathcal{A}}\left(-3\,\mu_n\,k^4\alpha^2 + 3\,\mu_p\,k^4 - 2\,c_2\,\omega^4 - 3\,k^4\beta\,\mu_p + 3\,k^2\beta\,\omega^2 c_1 + 12\,k^4\beta\,\omega^2 - 3\,k^4\beta\,\mu_n\,\alpha\right),$$

$$\Delta_4 = \frac{k}{2\omega^3\mathcal{A}}\left(-3\,\mu_n\,k^4\alpha^2 + 3\,\mu_b\,k^4\beta^2 + 2\,\mu_p\,k^4 - 2\,c_2\,\omega^4 - \mu_b\,k^4\beta + k^2\omega^2 c_1 + 4\,k^4\omega^2 - \mu_n\,k^4\alpha\right),$$

$$\Delta_5 = \frac{k\alpha}{2\omega^3\mathcal{A}}\left(2\,\mu_n\,k^4\alpha^2 - 3\,\mu_b\,k^4\beta^2 - 3\,\mu_p\,k^4 + 2\,c_2\,\omega^4 - k^4\alpha\,\mu_b\,\beta - k^4\alpha\,\mu_p + k^2\alpha\,\omega^2 c_1 + 4\,k^4\alpha\,\omega^2\right),$$

$$\Delta_6 = \frac{k\beta}{2\omega^3\mathcal{A}}\left(-3\,\mu_n\,k^4\alpha^2 + 2\,\mu_b\,k^4\beta^2 + 3\,\mu_p\,k^4 - 2\,c_2\,\omega^4 - k^4\beta\,\mu_p + k^2\beta\,\omega^2 c_1 + 4\,k^4\beta\,\omega^2 - k^4\beta\,\mu_n\,\alpha\right),$$

$$\Delta_7 = -\frac{1}{2\omega^2\mathcal{A}}\left(3\,\mu_n\,k^4\alpha^2 - 3\,\mu_b\,k^4\beta^2 - 3\,\mu_p\,k^4 + 2\,c_2\,\omega^4\right),$$

$$\Delta_8 = \frac{1}{V^2\mathcal{B}}\Big(2\,V^3 c_1\,k^3 - 2\,V^2\omega^3 c_2 - 2\,\mu_n\,k^3\alpha^2 V - \mu_n\,k^2\alpha^2\omega - \mu_n\,\alpha\,k^2\omega - 2\,\mu_n\,\alpha\,Vk^3 + k^2\beta^2\omega\,\mu_b$$
$$+ 2\,k^3\beta^2 V\mu_b - \mu_b\,\beta\,k^2\omega - 2\,\mu_b\,\beta\,Vk^3 + V^2 c_1\,k^2\omega\Big),$$

$$\Delta_9 = \frac{\alpha}{V^2\mathcal{B}}\Big(-2\,k^3\beta^2 V\mu_b - k^2\beta^2\omega\,\mu_b + 2\,k^3 V^3\alpha\,c_1 - 2\,k^3 V\alpha\,\mu_p - k^2\alpha\,\omega\,\mu_p - 2\,k^3 V\alpha\,\mu_b\,\beta - k^2\alpha\,\omega\,\mu_b\,\beta$$
$$+ k^2\alpha\,\omega\,V^2 c_1 + 2\,V^2\omega^3 c_2 - k^2\omega\,\mu_p - 2\,Vk^3\mu_p\Big),$$

$$\Delta_{10} = \frac{\beta}{V^2\mathcal{B}}\Big(-2\,\mu_n\,k^3\alpha\,\beta\,V - \mu_n\,k^2\alpha\,\beta\,\omega - 2\,\mu_n\,k^3\alpha^2 V - \mu_n\,k^2\alpha^2\omega - \beta\,k^2\mu p\,\omega + 2\,\beta\,k^3 V^3 c_1 + \beta\,k^2 V^2 c_1\,\omega$$
$$- 2\,\beta\,k^3\mu_p\,V - 2\,V^2\omega^3 c_2 + k^2\omega\,\mu_p + 2\,Vk^3\mu_p\Big),$$

$$\Delta_{11} = \frac{1}{V\mathcal{B}}\left(-2\,V^2\omega^3 c_2 - 2\,\mu_n\,k^3\alpha^2 V - \mu_n\,k^2\alpha^2\omega - \mu_n\,\alpha\,k^2\omega + k^2\beta^2\omega\,\mu_b + 2\,k^3\beta^2 V\mu_b - \mu_b\,\beta\,k^2\omega + V^2 c_1\,k^2\omega + 2\,Vk^3\mu_p\right),$$

$$\Delta_{12} = \frac{\alpha}{V\mathcal{B}}\left(-2\,k^3\beta^2 V\mu_b - k^2\beta^2\omega\,\mu_b - k^2\alpha\,\omega\,\mu_p - k^2\alpha\,\omega\,\mu_b\,\beta + k^2\alpha\,\omega\,V^2 c_1 + 2\,V^2\omega^3 c_2 - k^2\omega\,\mu_p - 2\,Vk^3\mu_p + 2\,\mu_n\,k^3\alpha^2 V\right),$$

$$\Delta_{13} = \frac{\beta}{V\mathcal{B}}\left(-\mu_n\,k^2\alpha\,\beta\,\omega - 2\,\mu_n\,k^3\alpha^2 V - \mu_n\,k^2\alpha^2\omega - \beta\,k^2\mu_p\,\omega + \beta\,k^2 V^2 c_1\,\omega - 2\,V^2\omega^3 c_2 + k^2\omega\,\mu_p + 2\,Vk^3\mu_p + 2\,k^3\beta^2 V\mu_b\right),$$

$$\Delta_{14} = -\frac{1}{V\mathcal{B}}\left(2\,\mu_n\,k^3\alpha^2 V + \mu_n\,k^2\alpha^2\omega + 2\,V^2\omega^3 c_2 - k^2\omega\,\mu_p - 2\,Vk^3\mu_p - 2\,k^3\beta^2 V\mu_b - k^2\beta^2\omega\,\mu_b\right),$$

$$\mathcal{A} = \left(-\mu_b\,k^2\beta - \mu_p k^2 + \omega^2 c_1 + 4k^2\omega^2 - \mu_n k^2\alpha\right),$$

$$\mathcal{B} = \omega^3\left(-\mu_b\,\beta + V^2 c_1 - \mu_p - \mu_n\,\alpha\right).$$

[1]I. D. Kaganovich, E. Starsev, S. Klaskey, and R. C. Davidson, IEEE Trans. Plasma Sci. **30**, 12 (2002).
[2]A. P. Misra and N. C. Adhikary, Phys. Plasmas **18**, 122112 (2011).
[3]E. Okutsu, M. Nakamura, Y. Nakamura, and T. Itoh, Phys. Plasmas **20**, 561 (1978).
[4]S. Moolla, R. Bharuthram, S. V. Singh, G. S. Lakhina, and R. V. Reddy, Phys. Plasmas **17**, 022903 (2010).
[5]D. Grésillon and F. Doveil, Phys. Rev. Lett. **34**, 77 (1975).
[6]G. Parks, L. J. Chen, M. McCarthy, D. Larson, R. P. Lin, T. Phan, H. Reme, and T. Sanderson, Geophys. Res. Lett. **25**, 3285, doi:10.1029/98GL02208 (1998).
[7]M. Temerin, K. Cerny, W. Lotko, and F. S. Mozer, Phys. Rev. Lett. **48**, 1175 (1982).
[8]T. Honzawa, Phys. Rev. Lett. **53**, 1915 (1984).
[9]H. Bailung, S. K. Sharma, and Y. Nakamura, Phys. Plasmas **17**, 062103 (2010).
[10]S. C. Sharma and M. W. Johnson, Med. Phys. **20**, 377 (1993).

[11]S. Guo, L. Mei, and W. Shi, Phys. Lett. A **377**, 2118 (2013).
[12]M. K. Deka, N. C. Adhikary, A. P. Misra, H. Bailung, and Y. Nakamura, Phys. Plasmas **19**, 103704 (2012).
[13]B. C. Kalita, R. Das, and H. K. Sarmah, Phys. Plasmas **18**, 012304 (2011).
[14]S. K. Sharma and H. Bailung, Phys. Plasmas **17**, 032301 (2010).
[15]S. I. Popel and K. Elsëser, Phys. Lett. A **190**, 460 (1994).
[16]R. Sabry, W. M. Moslem, and P. K. Shukla, Phys. Plasmas **16**, 032302 (2009).
[17]R. A. Gottscho and C. E. Gaebe, IEEE Trans. Plasma Sci. **14**, 92 (1986).
[18]S. V. Vladimirov, K. Ostrikov, M. Y. Yu, and G. E. Morfill, Phys. Rev. E **67**, 036406 (2003).
[19]K. Dittmann, C. Kullig, and J. Meichsner, Plasma Phys. Controlled Fusion **54**, 124038 (2012).
[20]Y. Ma, C. Wang, J. Zhang, J. Sun, W. Duan, and L. Yang, Phys. Plasmas **19**, 113702 (2012).
[21]Jyoti and H. K. Malik, Phys. Plasmas **18**, 102116 (2011).
[22]T. V. Losseva, S. I. Popel, A. P. Golub, and P. K. Shukla, Phys. Plasmas **16**, 093704 (2009).
[23]T. V. Losseva, S. I. Popel, A. P. Golub, Yu. N. Izvekova, and P. K. Shukla, Phys. Plasmas **19**, 013703 (2012).
[24]R. Sabry, W. M. Moslem, and P. K. Shukla, Plasma Phys. Controlled Fusion **54**, 035010 (2012).
[25]V. M. Vasyliunas, J. Geophys. Res. **73**, 2839, doi:10.1029/JA073i009p02839 (1968).
[26]M. Hellberg, R. Mace, and T. Cattaert, Space Sci. Rev. **121**, 127 (2005).
[27]C. Tsallis, J. Stat. Phys. **52**, 479 (1988).
[28]C. Kharif, E. Pelinovsky, and A. Slunyaev, *Rogue Waves in the Ocean* (Springer-Verlag, Berlin, 2009).
[29]N. Akhmediev, A. Ankiewicz, and J. M. Soto-Crespo, Phys. Rev. E **80**, 026601 (2009).
[30]N. Akhmediev, A. Ankiewicz, and M. Taki, Phys. Lett. A **373**, 675 (2009).
[31]W. M. Moslem, R. Sabry, S. K. El-Labany, and P. K. Shukla, Phys. Rev. E **84**, 066402 (2011).
[32]W. M. Moslem, Phys. Plasmas **18**, 032301 (2011).
[33]A. ur-Rahman, S. Ali, W. M. Moslem, and A. Mushtaq, Phys. Plasmas **20**, 072103 (2013).
[34]S. A. El-Tantawy, N. A. El-Bedwehy, and S. K. El-Labany, Phys. Plasmas **20**, 072102 (2013).
[35]A. Panwar, H. Rizvi, and C. M. Ryu, Phys. Plasmas **20**, 082101 (2013).
[36]A. Panwar and C. M. Ryu, Phys. Plasmas **21**, 062104 (2014).
[37]S. Guo, L. Mei, and A. Sun, Ann. Phys. **332**, 38 (2012).
[38]S. Guo and L. Mei, Phys. Plasmas **21**, 082303 (2014).
[39]H. Bailung, S. K. Sharma, and Y. Nakamura, Phys. Rev. Lett. **107**, 255005 (2011).
[40]S. K. Sharma and H. Bailung, J. Geophys. Res. **118**, 919, doi:10.1002/jgra.50111 (2013).
[41]T. Taniuti and N. Yajima, J. Math. Phys. **10**, 1369 (1969).
[42]N. S. Saini and I. Kourakis, Phys. Plasmas **15**, 123701 (2008).
[43]M. Onorato and D. Proment, Phys. Lett. A **376**, 3057 (2012).
[44]S. Sultana, G. Sarri, and I. Kourakis, Phys. Plasmas **19**, 012310 (2012).